LUND UNIVERSITY
Faculty of Science

Entanglement in a quantum heat engine

Harald Öhrn

Thesis submitted for the degree of Bachelor of Science
Project duration: 2 months, 15 hp

Supervised by Peter Samuelsson
Co-supervised by Björn Annby-Andersson

Department of Physics
Division of Mathematical Physics

June 2020

Abstract

In 2015 Jonatan Bohr Brask et al. showed that steady-state entanglement could be generated in two interacting qubits incoherently coupled to thermal baths of different temperatures [1]. This thesis is an attempt to re-evaluate their findings with the hope that a slightly different approach and system can help further our understanding of this not yet well understood phenomena. A Lindblad master equation approach is taken to study a two-qubit thermal machine interacting with bosonic thermal reservoirs. It is found that the steady-state entanglement behaves similarly using the Lindblad approach, the main difference being that a larger amount of entanglement can be generated than initially found in Ref. [1].

Acknowledgements

I would like to thank my supervisors Peter Samuelsson and Björn Annby-Andersson for making this thesis possible in more ways than one. Additionally, I thank my good friends Erik Wallin and Martin Jensen for proofreading the thesis. Lastly, special thanks to Patrick Potts for always answering any of my questions and for his invaluable comments on the report itself.

Contents

Chapter 1

Introduction

In 1824 Nicolas Léonard Sadi Carnot developed the Carnot-cycle, which describes how a series of temperature and pressure changes in an ideal gas can develop net mechanical work and in doing so laid the foundation for the second law of thermodynamics [2]. The Carnot-cycle describes a type of heat engine, a machine that converts a flow of thermal energy into mechanical energy. Another example of heat engines are the turbines in a nuclear or fossil fuel power plant that are a central part of modern electricity production. These kinds of heat engines are well understood in the framework of conventional thermodynamics. However, it is not yet well understood how heat engines behave when miniaturized since quantum mechanical effects become relevant.

Quantum mechanics describes the world on a microscopic scale, and it might appear contradictory to consider quantum effects in a heat engine, which historically is seen as a macroscopic system. In contrast, the current effort to establish the laws of thermodynamics in the quantum regime suggests a deeper connection between the two fields than what is intuitively apparent [3] [4]. The study of thermodynamical quantities such as heat, work and temperature on a quantum scale is called quantum thermodynamics. Of particular note is the quantum analogy to the heat engine, called a quantum heat engine.

A quantum heat engine is a microscopic system coupled to thermal reservoirs (or heat baths) where the resulting heat current produces a net amount of work, exactly as in a classical heat engine. The small size of the system makes it possible for quantum phenomena to appear. An example of such a phenomenon is quantum entanglement. In 2015 it was shown that steady-state entanglement could be generated in an autonomous thermal machine consisting of two qubits [1]. In

other words, the qubits could be entangled using only the temperature gradient, without any external control and in a stable configuration. This is a nice result as entanglement is necessary for several other applications in a variety of fields. It is, for example, required in quantum computation algorithms and for quantum teleportation [5].

This project will try to re-evaluate the results of Jonatan Bohr Brask et al. [1] using a similar, yet not identical, master equation approach. The Lindblad master equation was used instead of the Reset equation that was used in Ref. [1].

Chapter 2

Theory

2.1 Density matrices

Density matrices will be used extensively throughout this thesis, and as such, this section will contain a brief overview of their properties. Readers that are interested in a thorough formulation of the subject are referred to external material, such as Ref. [5]. Density matrices are a language for representing quantum mechanical states. They are used to describe statistical mixtures of states in a compact way.

The density matrix, usually denoted $\hat{\rho}$, contains all the information of the system it describes. It is defined as

$$\hat{\rho} = \sum_i p_i |\psi_i\rangle\langle\psi_i|, \tag{2.1}$$

where $0 \leq p_i \leq 1$ is the probability for the system to be in state $|\psi_i\rangle$. When the state $|\Psi\rangle$ of a system is known exactly, the system is said to be in a pure state and has the density matrix $\hat{\rho} = |\psi\rangle\langle\psi|$, otherwise it is in a mixed state. The density matrix is by definition a positive, Hermitian matrix with trace one, that is,

$$\begin{aligned} \hat{\rho}^\dagger &= \hat{\rho}, \\ Tr\{\hat{\rho}\} &= 1, \\ \langle \mathbf{\Psi}|\hat{\rho}|\mathbf{\Psi}\rangle &\geq 0, \forall \text{ vectors } |\mathbf{\Psi}\rangle. \end{aligned}$$

The density matrix for two uncorrelated system, here labeled 1 and 2, is given by the tensor product of the density matrices of the two separate system. For two

general two-dimensional subsystems this would be,

$$\hat{\rho}_{prod} = \hat{\rho}_1 \otimes \hat{\rho}_2 \tag{2.2}$$

$$\rightarrow \begin{bmatrix} a_1 & b_1 \\ c_1 & d_1 \end{bmatrix} \otimes \begin{bmatrix} a_2 & b_2 \\ c_2 & d_2 \end{bmatrix} = \begin{bmatrix} a_1a_2 & a_1b_2 & b_1a_2 & b_1b_2 \\ a_1c_2 & a_1d_2 & b_1c_2 & b_1d_2 \\ c_1a_2 & c_1b_2 & d_1a_2 & d_1b_2 \\ c_1c_2 & c_1d_2 & d_1c_2 & d_1d_2 \end{bmatrix}. \tag{2.3}$$

The state space of the product state is the tensor product of the state spaces of its parts [5]. For example, the product space of two qubits with basis $\{|0\rangle, |1\rangle\}$ has the basis $\{|00\rangle, |01\rangle, |10\rangle, |11\rangle\}$. Note that $|ab\rangle$ is short-hand for $|a\rangle \otimes |b\rangle$.

2.2 Entanglement and Concurrence

By definition, two particles, A and B, are said to be entangled if the total state $|\Psi\rangle$ of both particles cannot be described as a tensor product of the two separate states, i.e. $|\Psi\rangle \neq |\Psi_A\rangle \otimes |\Psi_B\rangle$. For example, the state $|\Psi\rangle = a_1b_1|u_1v_1\rangle + a_1b_2|u_1v_2\rangle + a_2b_1|u_2v_1\rangle + a_2b_2|u_2v_2\rangle$ describes two particles. Particle one can be in state $|u_1\rangle$ or $|u_2\rangle$ and particle two in $|v_1\rangle$ or $|v_2\rangle$. These particles are not entangled as $|\Psi\rangle = (a_1|u_1\rangle + a_2|u_2\rangle) \otimes (b_1|v_1\rangle + b_2|v_2\rangle)$. However, the state $c_1|u_1v_1\rangle + c_2|u_2v_2\rangle$ can not be separated in a similar fashion and therefore the two particles are entangled.

This definition of entanglement can be extended to mixed states as well. In general, a mixed state is said to be separable if it can be written as $\hat{\rho} = \sum_i w_i \hat{\rho}_i^A \otimes \hat{\rho}_i^B$, where ρ_i^A and ρ_i^B are mixed states on different subsystems A and B respectively and w_i are probabilities. As for pure states, a mixed state is considered entangled if it is not separable.

By this definition, a system is either entangled or not. It does not take into account varying degrees of entanglement; for this concurrence will be used. Concurrence is closely related to another, more general, measure of entanglement called entanglement of formation, but is only defined for systems consisting of a pair of qubits [6]. The concurrence is preferred in this project as it gives a clear metric for comparing entanglement levels of two states (a non-entangled state

has a concurrence of zero while a fully entangled state has concurrence one) and while the entanglement of formation has a better physical motivation the process of calculating it is beyond the scope of this project.

There exists an explicit formula for the concurrence C of a system [7].

$$C(\rho) = max\{0, \sqrt{\lambda_1} - \sqrt{\lambda_2} - \sqrt{\lambda_3} - \sqrt{\lambda_4}\}, \tag{2.4}$$

where λ_i are the eigenvalues of $\rho\tilde{\rho}$ in descending order. $\tilde{\rho}$ is the spin-flipped density matrix defined as

$$\tilde{\rho} = (\sigma_y \otimes \sigma_y)\rho^*(\sigma_y \otimes \sigma_y), \tag{2.5}$$

σ_y is the Pauli Y matrix and * denotes the complex conjugate.

2.3 Lindblad model/master equations

The non-unitary time evolution of a system that is in contact with its environment can be described with a differential equation called a master equation. Such a system is called an open system. The master equation should preserve the properties of the density matrix as given in Sec. 2.1. The most general form for Markovian master equations (systems without memory effects) is given by the Lindblad form as,

$$\frac{d\hat{\rho}}{dt} = -\frac{i}{\hbar}[\hat{H}, \hat{\rho}] + \sum_j \left[\hat{L}_j \hat{\rho} \hat{L}_j^\dagger - \frac{1}{2}\{\hat{L}_j^\dagger \hat{L}_j, \hat{\rho}\}\right]. \tag{2.6}$$

Here $\{a, b\} = ab + ba$ is the anti-commutator, $\hat{H}$ is the system Hamiltonian that describes the coherent part of the system dynamics and $\hat{L}_j$ are the Lindblad operators that describe how the system couples to its environment [5].

The reset model used in Ref. [1] derives a master equation from the assumption that during a short time interval the coupling to the thermal baths either resets the qubit to a thermalized state or leaves it unaffected [8][9]. In comparison the Lindblad master equation can be seen as a more physical approach, as it can be derived from microscopic theory. Ref. [10] provides such a derivation.

Chapter 3

System

3.1 The system

The system considered in this thesis is a thermal machine consisting of two coupled qubits, each coupled to a separate, bosonic, thermal bath, see Fig. 3.1. This particular system is chosen mainly because two-qubit systems allow for the use of concurrence. It also happens to be (one of) the smallest theoretically possible thermal machines [11], which limits the computational cost of solving the system.These two facets make this system ideal for studying entanglement generated by temperature gradients within the scope of this project.

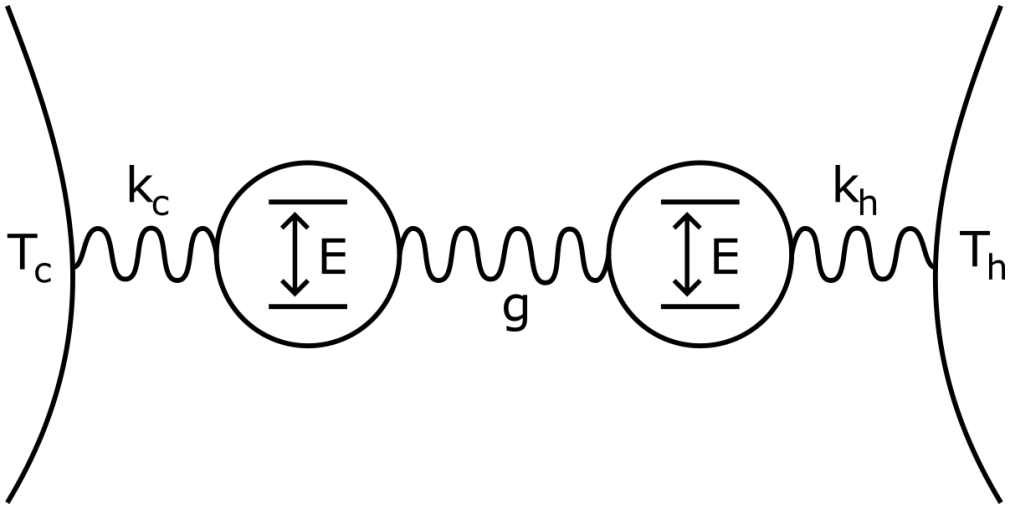

Figure 3.1: A sketch of the quantum thermal machine. Two qubits with energy gap E are coupled with a coupling constant g. The left qubit is coupled to a cold thermal bath of temperature T_c with a coupling constant k_c. Mirroring this, the right qubit is coupled to a hot thermal bath of temperature $T_h \geq T_c$ with constant k_h. The left qubit will be referred to as cold, with sub-index c and the right one as hot, with sub-index h.

3.2 The model

The time evolution of the state $\hat{\rho}$ of the two-qubit system can be described by the Lindblad master equation (2.6) and can be written as [3] [5] [12],

$$\frac{\partial \hat{\rho}}{\partial t} = i\left[\hat{\rho}, \hat{H}_0 + \hat{H}_{int}\right] + \mathscr{L}_c\hat{\rho} + \mathscr{L}_h\hat{\rho}, \tag{3.1}$$

where $\hat{\rho}$ is the density matrix and we set $\hbar = 1$ for the rest of this work. The term $i\left[\hat{\rho}, \hat{H}_0 + \hat{H}_{int}\right]$ describes the time evolution if the system was not coupled to the thermal baths. In the commutator, we have

$$\hat{H}_0 = E\left(|1\rangle\langle 1| \otimes \mathbb{1} + \mathbb{1} \otimes |1\rangle\langle 1|\right) \tag{3.2}$$

which is the free Hamiltonian and

$$\hat{H}_{int} = g\left(|10\rangle\langle 01| + |01\rangle\langle 10|\right) \tag{3.3}$$

which is the interaction Hamiltonian of the two qubits. The last two terms in Eq. (3.1) describe the interactions of the qubits with their corresponding bath and are given by

$$\mathscr{L}_\alpha \hat{\rho} = k_\alpha \left[r_\alpha + 1 \right] \left(\hat{\sigma}_\alpha \hat{\rho} \hat{\sigma}_\alpha^\dagger - \frac{1}{2} \{ \hat{\sigma}_\alpha^\dagger \hat{\sigma}_\alpha, \hat{\rho} \} \right) + k_\alpha r_\alpha \left(\hat{\sigma}_\alpha^\dagger \hat{\rho} \hat{\sigma}_\alpha - \frac{1}{2} \{ \hat{\sigma}_\alpha \hat{\sigma}_\alpha^\dagger, \hat{\rho} \} \right). \tag{3.4}$$

The operators $\hat{\sigma}_c = |0\rangle\langle 1| \otimes \mathbb{1}$ and $\hat{\sigma}_h = \mathbb{1} \otimes |0\rangle\langle 1|$ are defined as the lowering operators and $r_\alpha = \frac{1}{e^{E/T_\alpha} - 1}$ is the Bose-Einstein distribution, note that the Boltzmann constant k_B is set to one. In this work, we investigate the effects of keeping the system under a thermal bias while the chemical potentials of the reservoirs are set to be equal. Therefore, to simplify calculations, we can let the chemical potentials be zero without loss of generality. In principle one could look at the same effects for baths with different chemical potentials as in those with different temperature. However the non-conservation of photons requires the chemical potential to be zero, suggesting that a system with fermionic baths would be better suited for studying the effects of differing chemical potentials.

In Eq. (3.4) the $\hat{\sigma}_\alpha \hat{\rho} \hat{\sigma}_\alpha^\dagger$ term in the first parentheses describes how the qubit de-excites and the corresponding $\hat{\sigma}_\alpha^\dagger \hat{\rho} \hat{\sigma}_\alpha$ term in the second parentheses describes excitation of the qubit. The terms with the anti-commutators re-normalizes and makes sure that $\hat{\rho}$ keeps trace one.

The master equation holds in the perturbative regime $k_c', k_h', g << E$ and $k_c', k_h' << 1$ [1]. Note that k_α' is the coupling constant used if the system is described by the Fermi-distribution r_{FD} and is related to k_α as [3]

$$k_\alpha' = k_\alpha \frac{r(\frac{1}{T_\alpha})}{r_{FD}(\frac{1}{T_\alpha}))}. \tag{3.5}$$

To see that there exist equivalent forms using either Bose of Fermi-distributions consider that $r_{FD} = \frac{r}{1+2r}$. The equation would still describe the same system, irrespective to if one chooses to formulate it in terms of the Bose or Fermi-distribution.

3.3 Steady state solution

Of particular interest is the state when the system is static, that is, when the time derivative of Eq. (3.1) is zero. This is called the steady state solution. This can be done by re-writing Eq. (3.1) into matrix form using the basis $\{|00\rangle, |01\rangle, |10\rangle, |11\rangle\}$. Then wrap the density matrix into a vector $\boldsymbol{\rho}$ where the first four elements are the main diagonal, followed by the off-diagonal elements in order. Equation (3.1) can then be written in the form

$$\frac{\partial \boldsymbol{\rho}}{\partial t} = M\boldsymbol{\rho}, \tag{3.6}$$

where M is a $16x16$ matrix constructed by putting the factors for each differential equation into the rows of M, such that all the factors containing the first element of $\boldsymbol{\rho}$ are in the first column, all the factors containing the second element is in the second column and so on. The steady state solution is found by solving the system of equations $M\boldsymbol{\rho} = 0$, which corresponds to finding the null-space of M. The vector representation of the steady state can then be wrapped back to operator notation.

Manipulation of the master equation in matrix form was done in Mathematica 9 in the Wolfram language, including solving for the null-space of M. It should be noted that the non-diagonal part of M is quite sparse, allowing for computations to be done with reasonable speed. If this method would work for more complicated systems (increased number of baths or qubits, for example) depend in practice on the exact shape of M. Eventually the system would no longer be solvable analytically as is done here and one would be forced to consider other options, such as numerical solutions.

Chapter 4

Results

4.1 Steady state

The steady state solution is found as described in Sec. 3.3. In operator notation it is given by

$$\hat{\rho}_\infty = \gamma\left[k_c k_h \hat{\tau}_c \otimes \hat{\tau}_h + \frac{4g^2}{(k_c(1+2r_c)+k_h(1+2r_h))^2}(k_c\hat{\tau}_c + k_h\hat{\tau}_h)^{\otimes 2} + \frac{2g k_c k_h (r_c - r_h)\mathscr{Y}}{k_c(1+2r_c)+k_h(1+2r_h)}\right], \quad (4.1)$$

where $\hat{\tau}_\alpha = (r_\alpha + 1)|0\rangle\langle 0| + r_\alpha|1\rangle\langle 1|$. While the state $\hat{\tau}_\alpha$ is similar to a thermal state it is not a true thermal state in the sense that it is not normalized. This is not a problem in our discussion, but it is straight forward to re-write the solution using normalized thermal states. The constant $\gamma = (4g^2 + k_c k_h(1+2r_c)(1+2r_h))^{-1}$ is a normalization factor to ensure that the trace of $\hat{\rho}$ equals one, $\mathscr{Y} = i(|10\rangle\langle 01| - |01\rangle\langle 10|)$ and $A^{\otimes 2} = A \otimes A$ is the tensor square. Note that only two off-diagonal elements of the steady-state solution are non zero.

These results are in agreement with Ref. [3]. It should be noted that while the same calculations are present in Ref. [3] the approach for finding the solutions differ sightly. All results presented here have been calculated as described, given the Lindblad operators.

To check that the model gives us a proper physical state, the limits of high and low temperatures are calculated. Consider $T_c = T_h$, this would imply $r_c = r_h = r$. This in turn implies that the off-diagonal elements are both zero and that $\hat{\tau}_c = \hat{\tau}_h = \hat{\tau}$.

The steady state would then simplify to:

$$\begin{aligned}\hat{\rho}_\infty &= \frac{\hat{\tau}\otimes\hat{\tau}}{(1+2r)^2} \\ &= \frac{1}{(1+2r)^2}\left[|00\rangle\langle 00|(1+r)^2 + |01\rangle\langle 01|(1+r)r + |10\rangle\langle 10|(1+r)r + |11\rangle\langle 11|r^2\right]\end{aligned} \tag{4.2}$$

This limiting case is visualized in Fig. (4.1). In the low temperature limit ($T \to 0$), the steady state approaches $|00\rangle\langle 00|$. In the high temperature limit every state approaches equal probability. This is exactly what is expected of a four-level system in contact with a thermal bath.

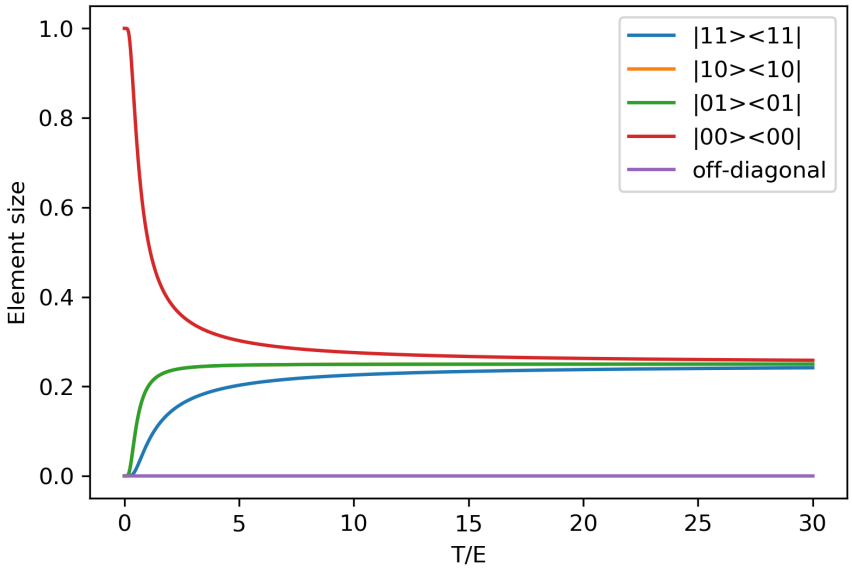

Figure 4.1: The elements of $\hat{\rho}$ where $T_c = T_h = T$ and the coupling parameters are fixed. $|10\rangle\langle 10|$ and $|01\rangle\langle 01|$ are identical over the entire interval and the off diagonal elements are zero. All main diagonal elements go asymptotically to 0.25 as the temperature goes to infinity.

4.2 ENTANGLEMENT

The steady-state solution (4.1) can be written in the form

$$\rho_\infty = \begin{bmatrix} a & 0 & 0 & 0 \\ 0 & b & if & 0 \\ 0 & -if & c & 0 \\ 0 & 0 & 0 & d \end{bmatrix}, \tag{4.3}$$

where a, b, c, d, f are real and positive (for $T_h > T_c$). The spin flipped state is given by Eq. (2.5) and reads

$$\tilde{\rho}_\infty = \begin{bmatrix} d & 0 & 0 & 0 \\ 0 & c & if & 0 \\ 0 & -if & b & 0 \\ 0 & 0 & 0 & a \end{bmatrix}. \tag{4.4}$$

Then

$$\rho_\infty \tilde{\rho}_\infty = \begin{bmatrix} ad & 0 & 0 & 0 \\ 0 & bc+f^2 & 2ibf & 0 \\ 0 & -2icf & bc+f^2 & 0 \\ 0 & 0 & 0 & ad \end{bmatrix} \tag{4.5}$$

with the eigenvalues

$$\lambda_i = \{ad, ad, (f-\sqrt{bc})^2, (f+\sqrt{bc})^2)\}. \tag{4.6}$$

The following relation was noted in Eq. (4.1): $ad - bc = -f^2$, which can be used to prove the inequalities

$$\sqrt{ad} < |f + \sqrt{bc}|, \tag{4.7}$$

$$f < \sqrt{bc}. \tag{4.8}$$

These inequalities together with

$$\{a, b, c, d, f\} > 0 \Longrightarrow |f - \sqrt{bc}| < |f + \sqrt{bc}|, \tag{4.9}$$

implies that $f + \sqrt{bc}$ is the square root of the largest eigenvalue. The absolute sign could be dropped and $|f - \sqrt{bc}| = \sqrt{bc} - f$ as a consequence of inequality (4.8). This in turn, gives the following expression for the concurrence from Eq. (2.4),

$$C(\rho_\infty) = max\{0, 2f - 2\sqrt{ad}\}. \tag{4.10}$$

The highest degree of entanglement possible to generate in the system was found by numerically maximizing Eq. (4.10) over g, k_c, k_h, T_c/E and T_h/E. This was done in Python using the L-BFGS-B minimization method provided by the scipy library. In the numerical calculations all parameters are given as a fraction of the separation of energy levels in the qubits. This makes them unitless if the units of Boltzmann's constant is taken into account. Figure (4.2. a) shows how the concurrence changes as the hot bath temperature increases. The concurrence finds its maximum value for the parameters: $g/E = 1.5285 \times 10^{-3}, k_c/E = 10^{-2}, k_h/E = 1.1374 \times 10^{-4}, T_c/E \approx 0$ (the numerical value used for low cold temperature was $T_c/E = 10^{-2}$ as going any lower would result in overflow errors) and $T_h/E = 8.1258$, all coupling constants were capped to 10^{-2} to make sure that the system is still in the perturbative regime. For these parameters the maximum concurrence is

$$C_{max}(\rho_\infty) = 0.0934. \tag{4.11}$$

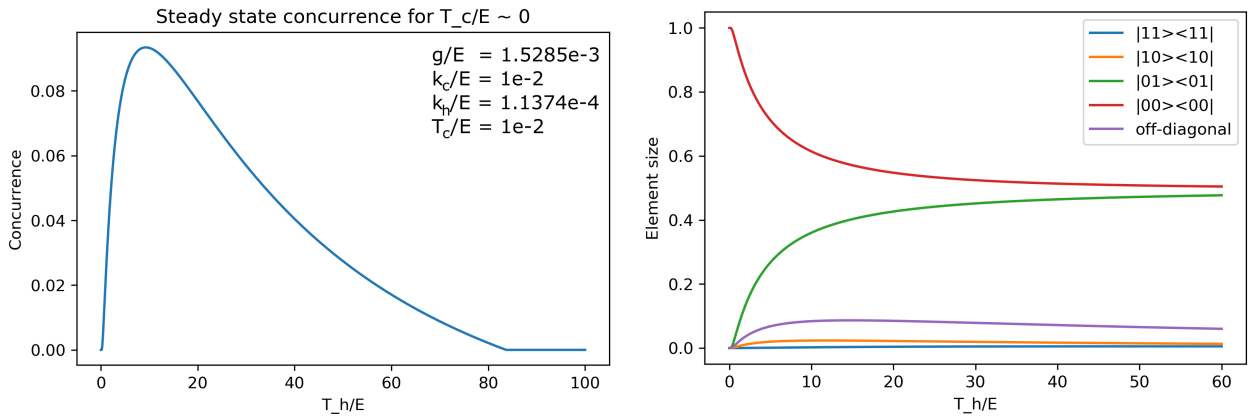

(a) **(b)**

Figure 4.2: (a): Concurrence generated in the steady state. The parameters g, k_c, k_h and T_c/E where optimized to give the highest peak value for the concurrence. (b): The individual, unique elements of $\hat{\rho}$, plotted with the same parameters as in (a), over a slightly shorter interval. The purple line shows the absolute value of the imaginary part of the two off diagonal elements. Note that the $|11\rangle\langle 11|$ element is not identically zero.

By keeping the coupling constants from Fig. (4.2) while varying the cold bath temperature it was observed in Fig. (4.3) that a minimum temperature difference is needed to generate concurrence, the size of this difference is dependant on the temperature of the cold bath in agreement with Ref. [1]. In addition, the maximal entanglement seems to decrease monotonically when the cold bath temperature is increased and for temperatures larger than approximately $T_c/E = 0.27$ no entanglement could be shown at all. The size of the individual elements of ρ_∞ are shown in Fig. (4.2. b). The figure visualizes the elements for the same parameters as in Fig. (4.2. a). In contrast to when both temperatures become large the density matrix tends towards an equal distribution between the ground state and the state where the hot qubit is excited while the cold one is not.

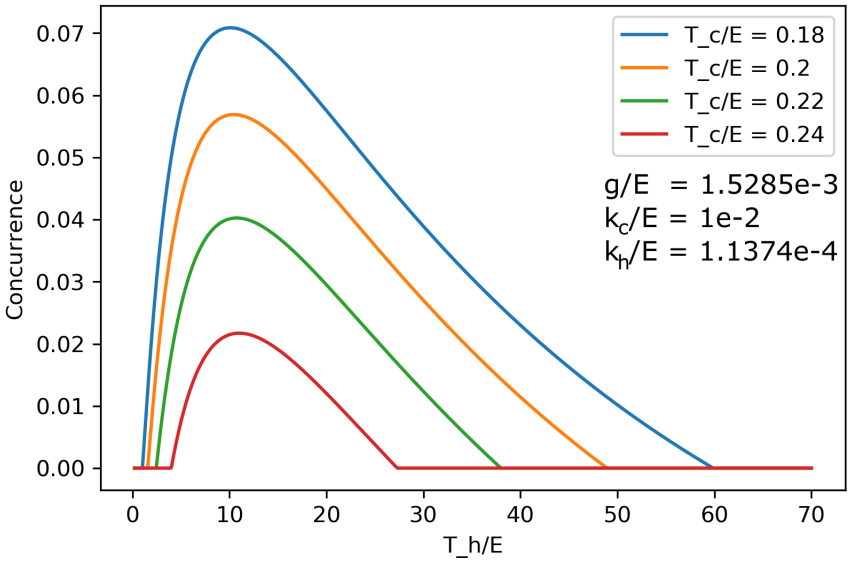

Figure 4.3: Concurrence as a function of hot bath temperature for several different cold bath temperatures. The parameters g, k_c and k_h are the same for each cold bath temperature and are not optimized again for the new fixed T_c/E.

Fig. (4.4) shows how the concurrence and the elements of the density matrix depend on g. It shows that for the same k_α, T_α as for peak concurrence in Fig. (4.2) the system is entangled for any non-zero g lower than a maximum value. In likeness to the behavior for increasing temperature difference, the concurrence quickly drops when g changes from its optimal value.

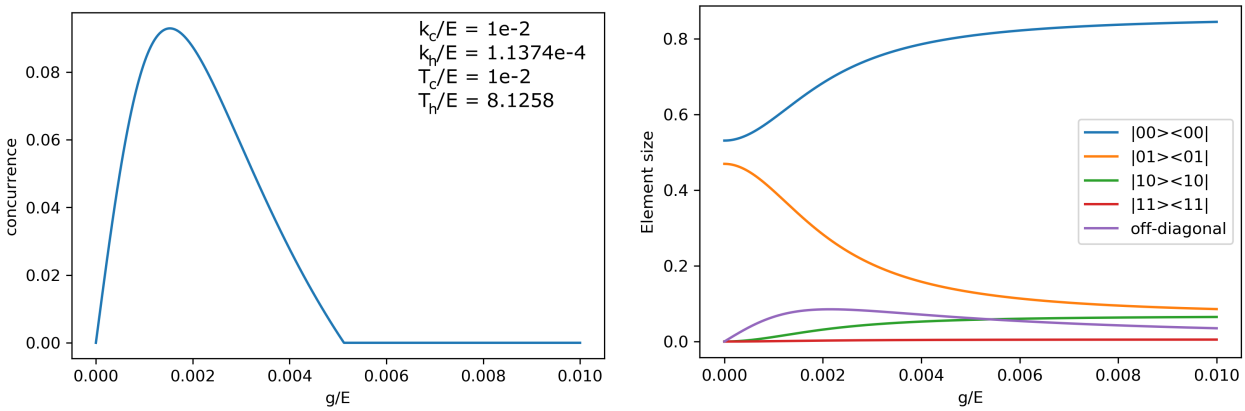

Figure 4.4: Concurrence generated in the steady state (a) and the elements of $\hat{\rho}_\infty$ plotted over the qubit to qubit coupling parameter g (b). The maximum value in (a) corresponds to the g used in Fig. (4.2).

Chapter 5

Conclusions

5.1 Discussion

The main results of Ref. [1] have been successfully replicated. Namely, entanglement can be generated in a two qubit thermal machine from entirely incoherent interactions with the heat baths, at the steady state. For the system to be entangled a minimum temperature difference and therefore heat current is required between the baths. In addition, the cold bath temperature must not be larger than some threshold value that depends on the separation of energy levels in the qubits. However, there are some differences between the results.

With the Lindblad model, we found the optimal temperature of the hot bath to generate maximal entanglement. This optimization would be very useful in an experimental realization of the system. To see why there is a suppression of the concurrence for high temperature notice that Eq. (4.1) could be re-written in terms of the Fermi-Dirac distribution, with a different coupling constant given by Eq. (3.5). This new coupling constant would then increase linearly at high temperatures; this is what causes the suppression.

With the Lindblad approach, the maximal entanglement is ca. 1.5 times larger in contrast to the approach using the reset model. There is also a difference for the threshold temperature for the cold bath where entanglement can no longer be generated. It is shown to be higher by a substantial margin, from $T_c/E \approx 0.21$ to $T_c/E \approx 0.27$.

In addition to the system considered here, Ref. [1] considers the same system with fermionic baths. In such a system entanglement can be generated for any large enough temperature difference, provided that the cold bath is colder than

the threshold temperature. In fact, with fermionic baths the system generates the largest amount of entanglement as $T_h \to \infty$. As the temperature difference grows one can imagine that keeping the cold qubit isolated from the hot bath could become a challenge. In contrast, the bosonic case would require much better control of the hot bath temperature.

It is hard to predict the exact effects of varying the parameters in the expression for the concurrence. However, some conclusions can be drawn from the above results. It should be noted that Eq. (2.4) was maximized with numerical methods and that it is its variations around this maximum that have been studied and as such tells us little of the functions behavior far from this maximum. It is found that of the three coupling constants, both g and k_h give maximum entanglement for values one or two magnitudes lower than the largest allowed value. This is nice when looking for maximal entanglement as they stay well within the weakly coupled regime. In contrast, the highest entanglement was found for k_c equal to the maximal value allowed to ensure that the models assumptions are correct. The comparison to Ref. [1] still holds true as the same assumptions about the coupling constants are made.

5.2 Outlook

It would be interesting to see if steady state entanglement can be created in different systems. Exploring the limits, both in terms of the strength of the coherence and the possible size of the entangled system, could determine the practical usefulness of incoherent entanglement generation for such things as quantum computation that may require large ensembles of entangled particles. Ref. [13] is a recent paper that concerns a similar topic, written by some of the same researchers that wrote the paper that inspired this thesis.

As in Ref. [14] one could investigate the fluctuations of entanglement in the system. For even if entanglement can be generated, if the fluctuations are as large or larger than the entanglement itself its usefulness in other applications could be severely limited.

Another possible direction to take is to study the heat currents through the

thermal machine. Calculating both the heat flow and its fluctuations could show how, if at all, entanglement impacts these quantities. With the end goal to study the thermodynamical uncertainty relation that relates the average energy flow, the average fluctuations of this flow and the created entropy in the system with each other. This would be done in the regime where the qubits are entangled. The validity of the thermodynamical uncertainty relation is in no way guaranteed in this case[15]. Arguably the most interesting outcome of such a study would be for the uncertainty relation to not hold in the presence of entanglement. For in that case it might be possible to devise ways to infer that a system is entangled by checking if the thermodynamical uncertainty relation holds or not.

Bibliography

[1] J. B. Brask, et al. *Autonomous Quantum Thermal Machine for Generating Steady-state Entanglement*, New J. Phys. **17** 113029 (2015).

[2] F. Ian, *Statistical Physics: an entropic approach* (John Wiley & Sons, Ltd., London, 2013), chap. 2

[3] P. P. Potts, *Introduction to Quantum Thermodynamics*, arXiv: 1906.07439v2 [quant-ph] (2019).

[4] F. Binder, L. Correa, C. Gogolin, J. Anders, G. Adesso, *Thermodynamics in the Quantum Regime*, Fundamental Theories of Physics, vol 195. Springer, Cham (2018) chap. 1-2

[5] M. A. Nielsen, I. L. Chuang, *Quantum Computation and Quantum Information* (Cambridge University Press, Cambridge, 2010), chap. 1-2 & sec. 8.4.1.

[6] W. K. Wooters, *Entanglement of formations and Concurrence*, QIC, Vol. 1, No. 1, **27-44** (2001).

[7] W. K. Wooters, *Entanglement of Formation of an Arbitrary state of two Qubits*, Phys. Rev. Lett. Vol. 80, No. 10 (1998).

[8] N. Linden, S. Popescu, P. Skrzypczyk, *How Small Can Thermal Machines Be? The Smallest Possible Refrigerator*, Phys. Rev. Lett. **105**, 130401 (2010).

[9] N. Linden, S. Popescu, P. Skrzypczyk, *The smallest possible heat engines*, arXiv:1010.6029v1 [quant-ph] (2010).

[10] G. Schaller, *Open Quantum Systems Far from Equilibrium* (Vol. 881, Berlin: Springer, 2014).

[11] N. Brunner, N. Linden, S. Popescu, P. Skrzypczyk, *Virtual qubits, virtual temperatures, and the foundations of thermodynamics* , Phys. Rev. E, Vol. 85, No. 5 (2012)

[12] P. P. Hofer, et al., *Markovian master equations for quantum thermal machines: local versus global approach*, New J. Phys. 19 123037 (2017)

[13] A. Tavakoli, G. Haack, N. Brunner, J. B. Brask, *Autonomous multipartite entanglement engines*, Phys. Rev. A **101**, 012315 (2020)

[14] E. B. Fel'dman, M. A. Yurishehev, *Fluctuations of Quantum Entanglement*, JETP Letters, vol. 90, No. 1, pp. 70-74 (2009).

[15] B. K. Agarwalla, D. Segal, *Assessing the validity of the thermodynamic uncertainty relation in quantum systems*, Phys. Rev. B **98**, 155438 (2018)